Journal of Molecular and Cellular Cardiology 45 (2008) 821–831

Contents lists available at ScienceDirect

Journal of Molecular and Cellular Cardiology

journal homepage: www.elsevier.com/locate/yjmcc

Original article

Marked differences between atrial and ventricular gene-expression remodeling in dogs with experimental heart failure

Sophie Cardin [a,c,1], Patricia Pelletier [a,b,1], Eric Libby [d], Sabrina Le Bouter [a], Ling Xiao [c], Stefan Kääb [e], Sophie Demolombe [f,g,h], Leon Glass [d], Stanley Nattel [a,b,c,*]

[a] Research Center and Department of Medicine, Montreal Heart Institute and Université de Montréal, Canada
[b] Department of Pharmacology, Université de Montréal, Canada
[c] Department of Pharmacology, McGill University, Montreal, Canada
[d] Department of Physiology, McGill University, Montreal, Canada
[e] Medical Hospital I, University of Munich, Germany
[f] INSERM, UMR915, l'Institut du Thorax, France
[g] CNRS, ERL3147, France
[h] Université de Nantes, Nantes, F-44000, France

ARTICLE INFO

Article history:
Received 26 June 2008
Received in revised form 12 August 2008
Accepted 12 August 2008
Available online 30 August 2008

Keywords:
Heart failure
Arrhythmias
Remodeling
Gene-expression
Metabolism
Fibrosis

ABSTRACT

Congestive heart failure (CHF) causes arrhythmogenic, structural and contractile remodeling, with important atrial–ventricular differences: atria show faster and greater inflammation, cell-death and fibrosis. The present study assessed time-dependent left atrial (LA) and ventricular (LV) gene-expression changes in CHF. Groups of dogs were submitted to ventricular tachypacing (VTP, 240 bpm) for 24 h or 2 weeks, and compared to sham-instrumented animals. RNA from isolated LA and LV cardiomyocytes of each dog was analyzed by canine-specific microarrays (>21,700 probe-sets). LA showed dramatic gene-expression changes, with 4785 transcripts significantly-altered ($Q<5$) at 24-hour and 6284 at 2-week VTP. LV gene-changes were more limited, with 52 significantly-altered at 24-hour and 130 at 2-week VTP. Particularly marked differences were seen in ECM genes, with 153 changed in LA (e.g. ~65-fold increase in collagen-1) at 2-week VTP versus 2 in LV; DNA/RNA genes (LA=358, LV=7); protein biosynthesis (LA=327, LV=14); membrane transport (LA=230, LV=8); cell structure and mobility (LA=159, LV=6) and coagulation/inflammation (LA=147, LV=1). Noteworthy changes in LV were genes involved in metabolism (35 genes; creatine-kinase B increased 8-fold at 2-week VTP) and Ca^{2+}-signalling. LA versus LV differential gene-expression decreased over time: 1567 genes were differentially expressed ($Q<1$) at baseline, 1499 at 24-hour and 897 at 2-week VTP. Pathway analysis revealed particularly-important changes in LA for mitogen-activated protein-kinase, apoptotic, and ubiquitin/proteasome systems, and LV for Krebs cycle and electron-transfer complex I/II genes. VTP-induced CHF causes dramatically more gene-expression changes in LA than LV, dynamically altering the LA–LV differential gene-expression pattern. These results are relevant to understanding chamber-specific remodeling in CHF.

1. Introduction

Congestive heart failure (CHF) is a leading cause of hospital admission and presently affects over 5 million Americans [1]. It is also one of the most important causes of atrial fibrillation (AF), the most common sustained cardiac arrhythmia [2]. Both pathologies are associated with important structural, electrophysiological, biochemical and molecular remodeling [3]. There are significant atrial–ventricular gene-expression differences [4], as well as differences between atrial and ventricular remodeling [5]. Ventricular gene-expression changes have been studied in dogs with terminal CHF caused by ventricular tachypacing (VTP) [6].

The VTP model of CHF produces a substrate for AF that reproduces many features observed in patients [7]. As in CHF patients, ventricular-tachypaced CHF dogs show time-dependent development of fibrosis, atrial and ventricular dilatation, and impaired ventricular and atrial function, as well as time-dependent electrophysiological remodeling manifested as ion-channel alterations and AF promotion [5,8–11]. In view of the different phenotypic features of atrial versus ventricular remodeling with the development of VTP-induced CHF [5], it is reasonable to consider the possibility that there may be chamber-specific patterns of gene-expression alterations. Furthermore, Barth et al. have shown that the atrial gene-expression pattern is changed in AF patients, becoming more similar to the ventricular gene-expression pattern [12]. Whether similar changes in chamber-specific gene-

* Corresponding author. Montreal Heart Institute, 5000 Belanger St. E., Montreal, Quebec, Canada, H1T 1C8. Tel.: +1 514 376 3330; fax: +1 514 376 1355.
E-mail address: stanley.nattel@icm-mhi.org (S. Nattel).
[1] S.C. and P.P. contributed equally to this study and share first authorship.

0022-2828/$ – see front matter © 2008 Elsevier Inc. All rights reserved.
doi:10.1016/j.yjmcc.2008.08.007

expression patterns occur in animal models of AF is unknown. The canine VTP-model allows for observations at different time points during the development of CHF, as well as the possibility to isolate purified cardiomyocyte preparations in order to obtain information about cardiomyocyte gene-expression with minimal contamination from other cell-types. This study was designed to use canine-specific microarrays to compare the evolution of atrial and ventricular gene-expression changes over 2 weeks of VTP, sufficient time to achieve the fully-developed AF substrate [13], as well as to determine whether chamber-specific gene-expression patterns are altered over this time.

2. Materials and methods

2.1. Animal model

Animal care procedures were approved by the animal-research ethics committee of the Montreal Heart Institute following guidelines of the Canadian Council for Animal Care. Experiments were performed on three groups of five mongrel dogs each, weighing 25–32 kg: 1 group each subjected to 24-hour or 2-week VTP, and a control sham-instrumented group. All groups were handled and followed as previously described [10,13,14]. A unipolar ventricular-pacing lead was inserted into the right-ventricular apex under 1.5%-halothane anesthesia and attached to a pacemaker in the neck. The pacemaker was programmed to pace at 240 bpm.

On study days, an ECG was recorded to confirm continued pacemaker-capture. Dogs were then anaesthetized (morphine, 2 mg/kg s.c.; α-chloralose, 120 mg/kg i.v. load; 29.25 mg/kg/h maintenance infusion) and ventilated. Arterial and left-ventricular (LV) end-diastolic pressures were measured with fluid-filled catheters.

Dogs were then euthanized by pentobarbital overdose, hearts were removed and placed in Tyrode solution aerated with 100% O_2. Left-atrial (LA) and left-ventricular (LV) free walls were removed and perfused via coronary arteries as previously described [14,15]. Cell isolation was performed on full-thickness free-wall samples via collagenase digestion. Cell pellets were then snap-frozen and stored at −80 °C.

2.2. RNA extraction

Cell pellets were immersed into Trizol (1 mL/100 mg of pellet) and pulverised. Samples were centrifuged at 8000 rpm, 15 min, and 4 C. The aqueous phase was transferred, added to an equal volume of chloroform and centrifuged (5 min, 8000 rpm, 4 C). The resulting aqueous phase was added to an equal volume of isopropanol, incubated (−20 C, 45 min) and centrifuged (8000 rpm, 5 min, 4 C). Pellets were centrifuged in ethanol, then re-suspended in 70% ethanol and incubated overnight (−20 C). Samples were then re-centrifuged (13,000 rpm, 5 min, 4 C) and pellets dried and resuspended in DEPC water. RNA concentrations were characterized on RNA 6000 nano-chips (Agilent 2100 Bioanalyzer). Samples with 260/280 nm OD ratios <1.8 were rejected.

2.3. Microarray processing and analysis

Fragmented cRNA (10 μg) was hybridized to Affymetrix GeneChip Canine Genome Arrays (23,836 probe-sets detecting 21,700 transcripts) with Affymetrix GeneChip one-cycle target labeling and control reagents kits. One microarray was used for each tissue sample for each dog. Thus, since 3 groups of 5 dogs each were studied and 2 tissue samples (one from LA and from LV) were analyzed for each dog, results from a total of 30 microarrays were used. GeneChip Fluidics Station 450 was used to stain and wash the chips, followed by visualization on an Affymetrix GeneChip Scanner 3000.

Microarray expression data from each of the 30 chips studied were subjected to Invariant Set Normalization in dChip to correct inter-array difference in average brightness. The dChip algorithm was also used to calculate the Model Based Expression Index to integrate probe intensities into one representative expression-value/gene. Multiple (~11) pairs of probes were used to measure the level of transcription of each sequence represented on the array. As set, dChip detected and rejected single, probe, and array outliers, using only the intensities of perfect-match probes for analysis. Canine-specific genes representing adrenergic-receptors, glucose-6-phosphatase, and glyceraldehyde-3-phosphate were employed as on-chip controls. Significance Analysis for Microarrays (SAM) was used to identify differentially expressed genes in VTP versus sham comparisons at q-values <5, implying that <5% of genes identified as differentially expressed would be false positives (equivalent to a P-value cut-off of $P<0.05$). Since there was an extremely large number of atrial–ventricular gene differences, we reduced the q-value for the atrial–ventricular comparison analysis to 1, to decrease false-positive identifications to <1% (equivalent to a P-value of $P<0.01$) and have a more tractable data set.

Genes without Affymetrix annotations were BLAST-searched for mammalian sequence-homologies with E-value $<10^{-4}$. For functional annotations, we used Affymetrix's human-to-canine gene-mapping and the human Gene Ontology (GO) database. Genes that could not be identified by this process were classified by literature search.

2.4. Real-time RT-PCR

Real-Time RT-PCR (Gene Amp 5700, Perkin-Elmer) was used to confirm microarray data for 19 selected genes. First-strand cDNA was synthesized from 2 μg total RNA (High Capacity cDNA Archive Kit, Applied Biosystems). On-line PCR was performed (duplicate analyses for each sample) with FAM-labeled fluorogenic TaqMan probes and primers (Assay-by-design, Applied Biosystems). Target-gene signals were normalized to 18S-ribosomal RNA-values. Primers and probe sequences are provided in On-line Table 1. Data were analyzed with the comparative threshold cycle (Ct) relative-quantification method.

2.5. Western blot analysis

Protein-expression for 8 selected genes was analyzed by Western Blot. Protein samples (100 μg) were subjected to SDS-polyacrylamide gel electrophoresis, transferred to nitrocellulose or PVDF membranes and incubated with antibodies listed in Online Table 2. Bands were quantified with QuantityOne software and normalized to GAPDH band-intensities on the same samples.

2.6. Pathway analysis

Gene network pathways were derived from GenMapp (Gene Map Annotator and Pathway Profiler), a free computer application available at www.genmapp.org designed to visualize gene-expression data on maps representing biological pathways and groupings of genes [16]. GenMapp 2.1 canine maps are homology maps derived from human-based maps and include 42 cellular, 27 metabolic, 11 molecular and 15 physiological process maps. The microarray dataset containing genes for each LA and LV VTP transcript with statistically-significant changes (q-value <5.0, listed in Online Table 3) were uploaded on an Excel spreadsheet containing identifiers (*Entrez gene*) and corresponding expression values. The raw data file was then converted via Expression Dataset Manager into a GenMAPP Expression Dataset format (.gex). Analysis was based on GenMAPP Gene Database canine-specific library Cf-Std_20070517.gdb, downloaded from www.genmapp.org. All the maps were applied and pathways containing multiple VTP-induced gene-expression changes of interest were retained for study/illustration. These maps were redrawn for data presentation with Microsoft PowerPoint 2007, with additional genes added based on KEGG (http://www.genome.jp/kegg) and Reactome (http://reactome.org/) websites.

Table 1
Hemodynamic changes

	Sham	24-hour VTP	2-week VTP
Pressures (mmHg)			
Systolic-arterial	136±7	109±16*	108±15*
Diastolic-arterial	90±5	68±9*	70±12*
LV end-diastolic	1±1	5±2	16±5**

*$P<0.05$, **$P<0.01$ versus sham.

2.7. Statistics

Data are shown as mean±SEM. All samples were studied as individual tissue samples from individual dogs: no sample pooling was performed. Comparisons were performed with analysis of variance (ANOVA) and Tukey's test.

3. Results

VTP caused a decrease in arterial pressure and increase in LV end-diastolic pressure at 2 weeks (Table 1). At 2 weeks, all dogs had ascites, visibly dilated hearts and pulmonary congestion.

3.1. VTP-induced changes relative to sham

A detailed list of all genes showing statistically-significant differences for at least one analysis is provided in On-line Table 3. Relative to sham dogs, 4785 LA genes were differentially expressed by 24-hour VTP and 6284 by 2-week VTP. In contrast, 52 were differentially expressed in the LV at 24-hour VTP and 130 at 2-week VTP. Fig. 1 shows mean mRNA expression indices for each transcript versus corresponding sham values for each group of dogs. Red points indicate statistically-significant changes versus sham, blue points indicate values that were not significantly different between groups. A full listing of relative expression values, Gene IDs and annotations is provided for all LA and LV VTP transcripts with statistically-significant changes in Online Table 3.

Fig. 2 shows the number of significantly up-and down-regulated genes in each functional category. In LA, there were almost equal numbers of genes up-and down-regulated at 24-hour VTP (45% down, 55% up) and in 2-week VTP (50% down, 50% up). In contrast, most of the significant LV changes consisted of down-regulation at 24-hour VTP (88% down, 12% up), a predominance that remained but was less striking at 2 weeks (68% down, 32% up). Substantial changes were seen for all gene groups in LA, but particularly large numbers of changes were seen in DNA/RNA synthesis and degradation, metabolism, protein synthesis and degradation, and signal transduction.

Although the numbers of genes changed were much greater in LA than LV, the relative numbers of up- versus down-regulated genes were often similar for both. For example, at 2-week VTP gene categories with more up- than down-regulated genes in LA included cell cycle and growth (96 up/63 down), immunity (121 up/26 down), and cell structure and mobility (97 up/62 down). Corresponding results for LV were 3 up/1 down, 1 up/0 down, and 4 up/2 down. For ECM genes, 124 were upregulated and 29 down in LA after 2-week VTP, compared to 1 gene each up- and down-regulated in LV. Other gene-classes showed more down-regulated than upregulated genes after 2-week VTP, once again with parallel patterns in LA and LV: metabolism-related genes (LA: 175 up/306 down, LV: 4 up/31 down) and DNA and RNA synthesis (LA: 117 up/241 down, LV: 2 up/5 down). Finally, some gene categories showed similar numbers of up- and down-regulated genes, e.g. signal transduction genes, with LA: 215 up-regulated and 205 down-regulated after 2-week VTP, LV: 8 up/8 down. For most gene groups, the relative portion of up- versus down-regulated genes was

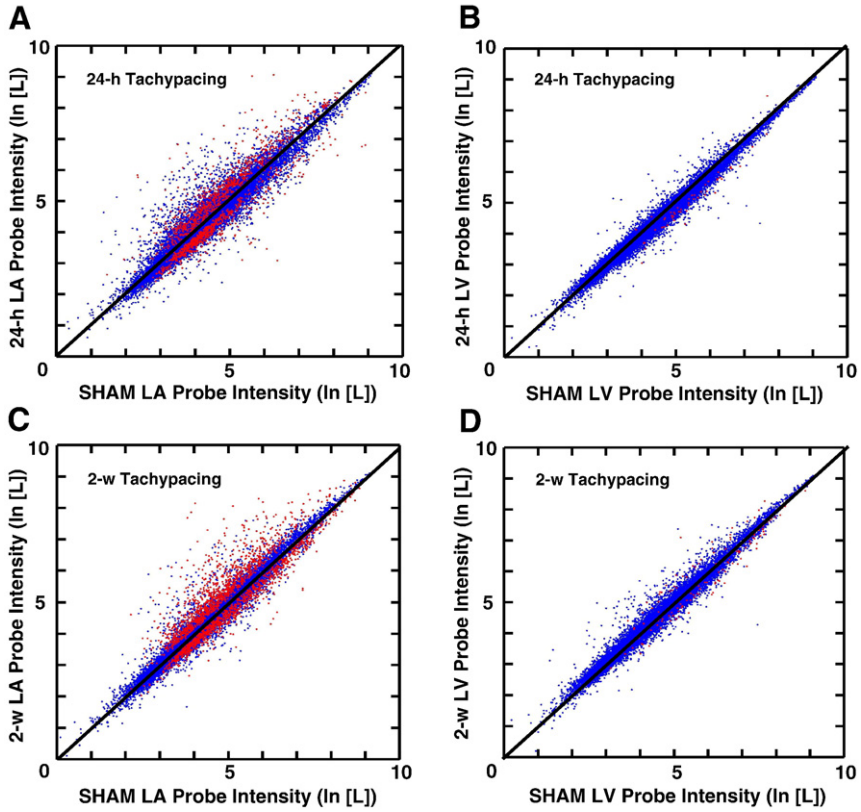

Fig. 1. Overall mRNA expression-changes compared to sham at 24-hour VTP in LA (A) and LV (B), and at 2-week VTP in LA (C) and LV (D) samples. The relative probe intensity, in $\log_e$ (L), where L=mean sample luminescence, of each intervention-group gene is plotted as a function of the corresponding value for the VTP-sham group gene and represented as a single point. Red points are significantly different from sham-controls ($Q<5$) whereas blue points are not significantly different. Without any changes in mRNA expression, all points would fall on the black line of identity.

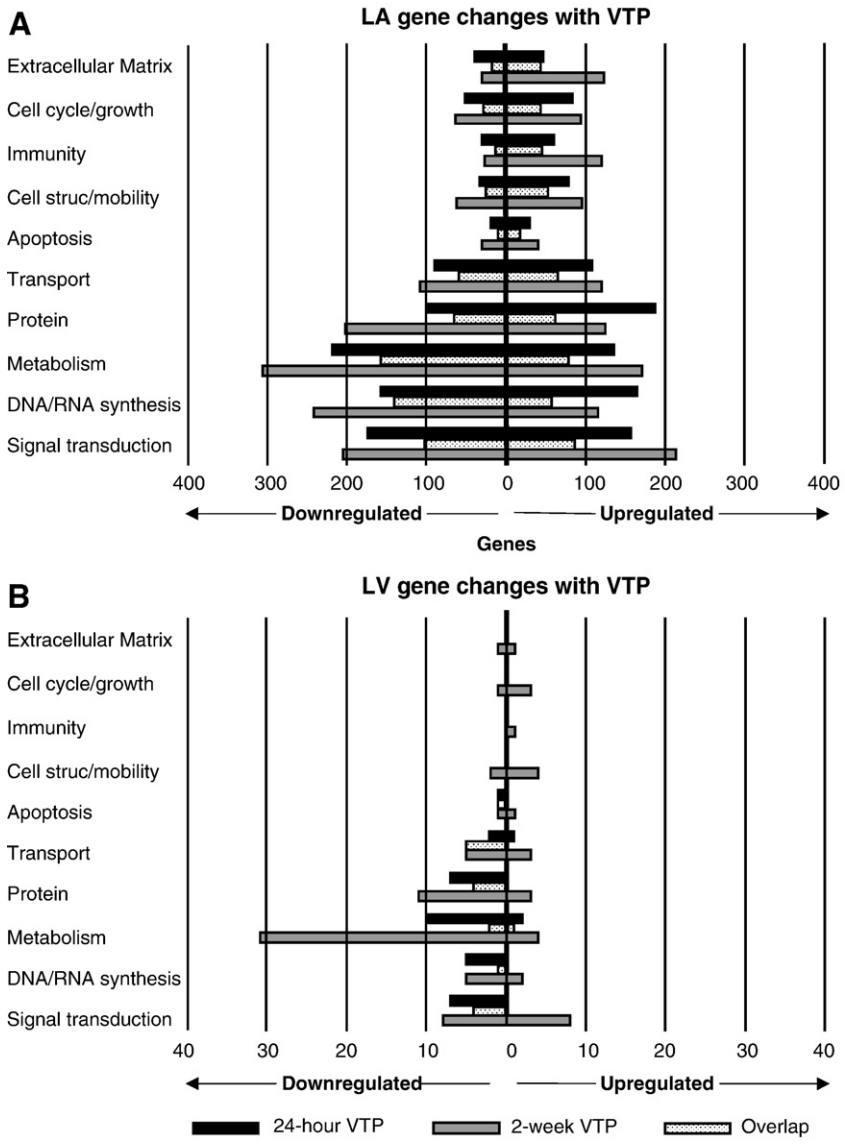

Fig. 2. Total number of genes of each functional group for which mRNA expression was significantly changed. Graph shows respective number of genes down-or up-regulated by ventricular–tachycardia remodeling in atria (A) or ventricles (B). "Overlap" refers to the number of genes that were significantly affected in the same direction at both 24 h and 2 weeks of tachypacing.

qualitatively similar for 24-hour and 2-week VTP. A notable exception was protein synthesis and degradation, for which about twice as many LA genes were up-versus down-regulated at 24 h (190 versus 97 respectively), whereas the ratio was inverted at 2 weeks (126 up/201 down).

Large LA–LV differences were observed in relation to ECM-gene-expression. Many important ECM genes showed large statistically-significant changes in LA without statistically-significant changes in LV. For example, 16 probe-sets corresponding to 12 transcripts encoding collagen-related genes were significantly increased in the LA at 2-week VTP. Particularly impressive differences occurred in collagen-1/alpha-1 (~65-fold increase versus sham in LA), collagen-3/alpha-1 precursor (~20-fold increase versus sham), and collagen-1/alpha-2, collagen-5/alpha-1 and collagen-12/alpha-2 (all increased ~10-fold). The large LA–LV differences in these collagen genes and the fact that most of the collagen-gene-expression increases were significant in LA at 2-week but not 24-hour VTP agrees well with the time-course and magnitude of fibrosis in the 2 chambers [5]. Additional differential ECM-gene-changes of interest included those in fibronectin (significant, ~11-and 16-fold increases in LA at 24-hour and 2-week VTP respectively), elastin (~10-fold at 2-weeks), fibrillin-1 (~2.5 and ~8-fold at 24-hour and 2-week VTP), TIMP-1 (~6-fold increased at 24-hour and 2-week VTP) and TIMP-3 (50%-decreased at 24-hour VTP).

Although relatively few genes were significantly altered in LV, some interesting patterns emerged. The most affected categories were signal transduction, protein synthesis and degradation, and in particular, metabolism. A number of respiratory-chain complex genes were down-regulated at 2-week VTP in LV, including NADH dehydrogenase Fe-S protein 8 (35% decrease versus sham), succinate dehydrogenase (25% decrease), and ubiquinol-cytochrome oxidoreductase (25% decrease). Other metabolism-related genes that were significantly and prominently decreased at 2-week VTP in LV included glutathione-transferase (~60% decrease), NADH-ubiquinone oxidoreductase 30-kDa subunit (~30%), succinate-dehydrogenase precursor (~20%), and succinate-CoA ligase (~25%). Interestingly, creatine-kinase was significantly up-regulated >8-fold in LV at 2-week VTP, versus ~5-fold in LA at the same time point. Two genes encoding proteins involved in Ca^{2+}-related arrhythmogenesis were significantly up-regulated in LV at 2-week VTP: calmodulin (types 1

and 3 increased ~40 and 90% respectively) and FKBP12 (increased ~70%).

3.2. Evolution of LA–LV expression profile differences

Fig. 3 compares the mean value of mRNA expression levels for all transcripts in LA versus LV, based on paired samples obtained from each dog at each time point. Blue points indicate non-significant differences between LA versus LV while values in red are significantly-different (q-value<1). In the sham group, 1567 genes were differently expressed in LA versus LV, while 1499 were differential at 24-hour VTP and 897 at 2-week VTP. Detailed results are presented in Online Table 3. In the sham group, almost as many genes showed lower-level expression as higher-level in LA versus LV (53% versus 47%). At 24-hour VTP, fewer genes showed lower-level expression in LA (44% lower and 56% higher) and this difference increased further at 2-week VTP (33% lower-level and 66% higher-level in LA than LV). Thus, although the number of LA–LV gene-expression differences decreased with VTP, their pattern changed, with an increasing proportion becoming attributable to genes upregulated in LA.

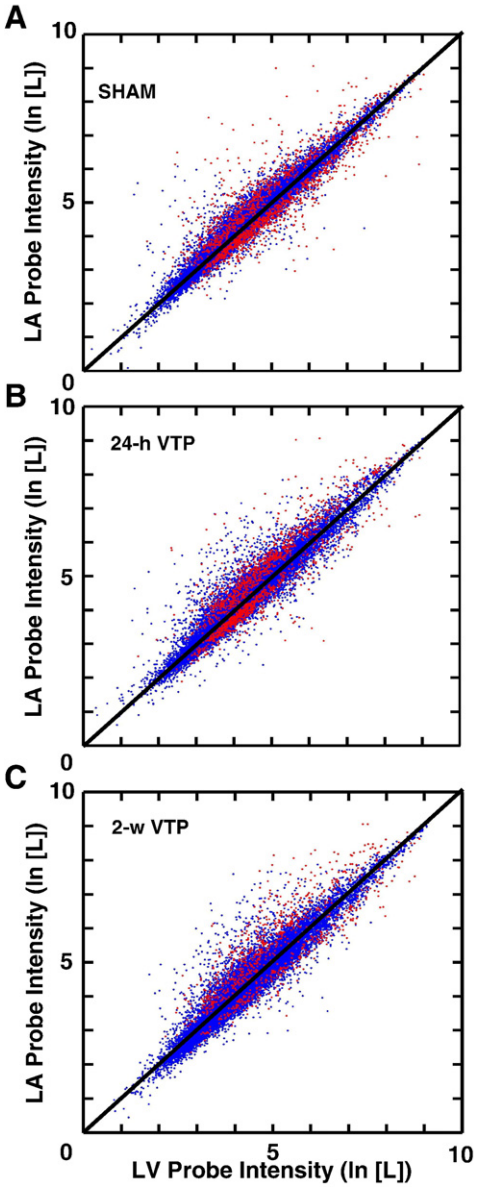

Fig. 3. Differences in mRNA expression in LA compared to LV in shams (A), 24-hour VTP (B), and 2-week VTP (C) samples. Format as in Fig. 1. The relative probe intensity, in $\log_e$ (L), where L=mean sample luminescence, of each intervention-group gene is plotted as a function of the corresponding value for the VTP-sham group gene and represented as a single point. Red points are significantly different from sham-controls whereas blue points are not significantly different. Without any changes in mRNA expression, all points would fall on the black line of identity.

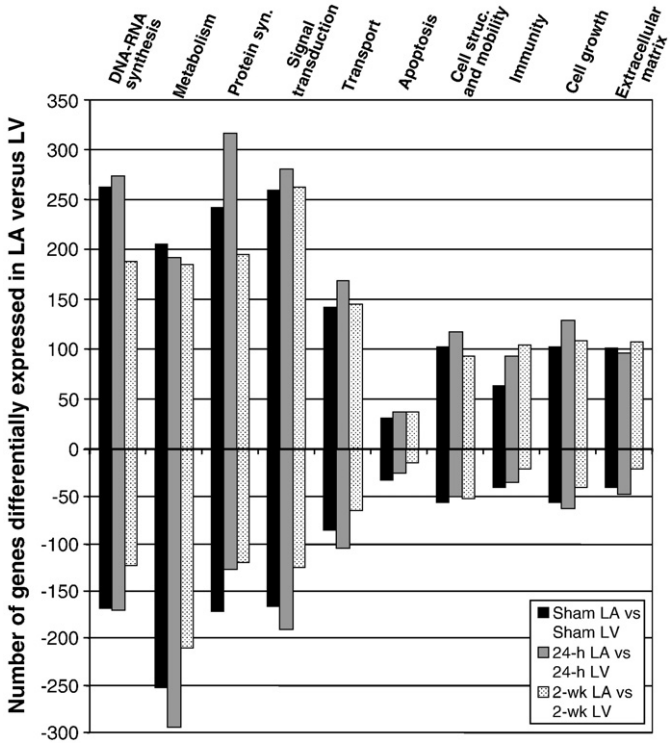

Fig. 4. Total number of genes of each functional group for which levels were significantly different in LA versus LV in shams, 24-hour VTP or 2-week VTP.

The temporal evolution of LA–LV differentially expressed gene groups is illustrated in Fig. 4. For a number of gene groups differently expressed in LA versus LV, differences tended to increase after 24-hour VTP and then to decrease after 2 weeks: e.g. DNA and RNA synthesis (430 differential genes in shams, 444 at 24-hour VTP, 311 at 2-week VTP); metabolism (sham: 458; 24-hour VTP: 487; 2-week VTP: 395); protein synthesis and degradation (sham: 414; 24-hour VTP: 443; 2-week VTP: 315); signal transduction (sham: 425; 24-hour VTP: 482; 2-week VTP: 387); transport (sham: 227; 24-hour VTP: 273; 2-week VTP: 210). For most gene categories, these changes were equally distributed between increased and decreased expression-level in LA compared to LV for each time point. Immunity-related genes showed a somewhat different pattern (sham: 103; 24-hour VTP: 127; 2-week VTP: 124), with differential genes remaining increased at 2-week VTP.

3.3. Real-time PCR results

Quantitative real-time PCR was performed on 18 genes for each group of dogs. Genes believed to be of pathological importance were selected to represent over-expressed, under-expressed or nonsignificantly-changed genes. Fig. 5 compares gene-expression levels by real-time RT-PCR with microarray results, which showed a good correlation (R^2=0.90). Detailed results are presented in Table 2. Of the 76 values obtained by real-time RT-PCR, 76% (57) showed concordant statistical significance or non-significance with microarray analysis. Over 97% (74) of the sample-sets showed changes in the same direction with both methods. Thus, there was good agreement overall.

3.4. Western-blot results

Western-blot analysis was performed on 8 selected proteins. Fig. 6 presents representative blots. Table 3 compares the mean results of

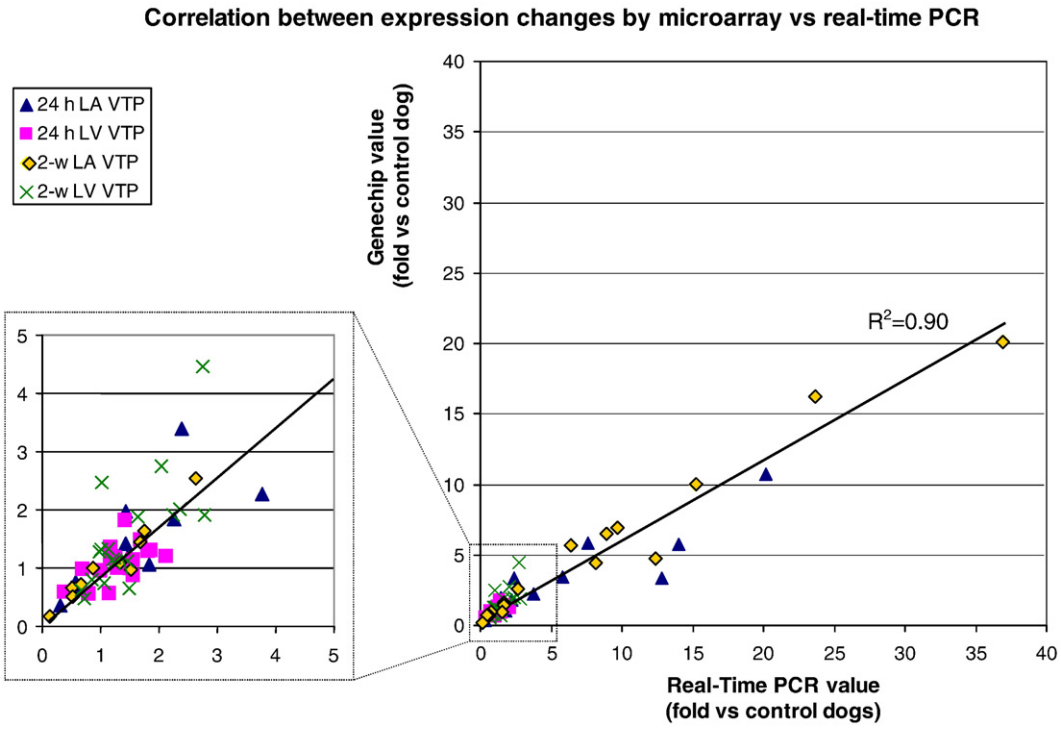

Fig. 5. Correlation between expression changes by real-time PCR versus microarray for each sample, for each of 18 genes. Regression lines are shown. Many points are clustered in the <5-fold-change range, which is therefore shown on an expanded scale at the left.

Western-blot analysis to corresponding microarray findings. Statistical congruence (significant changes in the same direction for both protein and mRNA or no significant change in either) was seen for 23/32 (72%) of data sets. Of the remaining 9 cases of statistical non-convergence (significant for one but non-significant for the other), the values for 6 of them were of the order of ±25% of each other. Although there was good overall and qualitative agreement between mRNA expression and protein expression changes, some quantitative differences existed, particularly for secreted proteins (e.g. IL1-Ra and collagen-3 alpha-1 chain show larger mRNA than protein changes).

3.5. Pathway analysis

Pathway analysis revealed VTP-induced changes for important numbers of genes in 3 signalling pathways, involving mitogen-activated protein kinases (MAPKs), apoptotic signalling, and the ubiquitin–proteasome system. Consistent with the very limited number of ventricular genes affected by VTP, all the signalling pathways highlighted pertained to atrial-gene signalling. In addition, 3 metabolic pathways were highlighted, including respiratory-chain enzymes, the Krebs cycle, and glycolysis. Of note, two of these (Krebs cycle and electron-chain transfer) involved significant changes at the ventricular level.

Previous work suggests a significant role for the MAPKs ERK, p38 and JNK in CHF-related atrial remodeling [5,13,17]. LA changes in MAPK-signalling genes highlighted by pathway analysis are shown in On-line Fig. 1. VTP-induced up-regulation was evident for key signalling enzymes such as MAPK1 (encoding ERK2), MAPK14 (p38α) and MAPK11 (p38β). Interestingly, previous work [17] showed that significant changes in atrial p38-protein expression occur within 24 h while ERK changes more slowly (reaching statistical significance at 1-week VTP), in keeping with our observation of significant atrial p38-encoding mRNA upregulation at 24 h and ERK-encoding changes occurring only at 2 weeks in the present study. Upstream activators of MAPK signalling are upregulated in the LA early in VTP-remodeling, notably including the small G-protein signalling elements RAC1 (showing a 3.7-fold increase at 24-hour VTP) and the RAS-related genes SHC1 and HRAS.

Another gene-pathway that showed interesting changes was apoptotic signalling. Previous studies indicated that atrial apoptotic markers rise strikingly within 24 h of VTP-onset and decrease thereafter [5,11]. The changes in apoptosis-regulating systems that we observed are shown in On-line Fig. 2. The BCL2L1 gene, encoding an anti-apoptotic member of the Bcl-2 family, was up-regulated in LA after two weeks of tachypacing. Caspase-4, implicated in the response to endoplasmic reticulum stress [18], and calpain 2, but not calpain 1, were also upregulated after 24 h of VTP. In contrast, the death-associated protein-encoding gene DAXX [19] is strongly down-regulated after 24-hour VTP, pointing to the activation of counter-regulatory measures to limit apoptosis.

In addition to transcript changes encoding apoptotic proteins *per se*, we noted important alterations in the ubiquitin–proteasome system (On-line Fig. 3), which regulates apoptosis [20,21]. The most prominent changes occurred in the LA after 24-hour VTP, with fewer alterations at 2 weeks and no statistically-significant changes in the LV. At 24-hour VTP, 6 LA genes in the E2-ubiquitin conjugating enzyme system were altered (5/6 upregulated) and 3 genes in the E3-ligase system. Both 19S and 20S proteasome components of the 26S proteasome complex showed significant alterations. Two genes encoding lid subunits and 6 encoding base subunits of the 19S proteasome were upregulated in LA at 24-hour VTP, and 7 genes in the 20S proteasome were upregulated.

In contrast to the other pathways that we assessed, which showed virtually no significant LV changes, there were significant alterations in metabolic systems, principally in the Krebs cycle (On-line Fig. 4) and electron-chain transport (On-line Fig. 5). ACO2 encodes aconitase, which catalyzes the transformation of citrate into isocitrate in the Krebs cycle and SUCLG1 encodes succinate-CoA ligase: both were significantly down-regulated in LV tissue after 24-hour and 2-week VTP, whereas fumarate hydratase was down-regulated in LA. Many

Table 2
Comparison between mRNA expression fold-changes by microarray versus TaqMan real-time RT-PCR

	Gene ID	24-hour LA		2-week LA		24-hour LV		2-week LV	
		Real-Time	Gene chips	Real-Time	Gene chips	Real-Time	Gene chips	Real-Time	Gene chips
Signal transduction									
Calmodulin	1604374	1.46±0.17	0.99±0.02	1.68±0.20	1.19±0.12*	1.80±0.46	1.27±0.11	2.24±0.48	1.89±0.11*
Apoptosis									
p53	1582452	1.83±0.44	1.06±0.05	1.52±0.24	0.97±0.05	1.25±0.32	1.16±0.05	1.46±0.26	1.12±0.09
Cathepsin S	1582636	14.02±5.36	5.71±1.65*	9.64±4.19	6.98±1.75*	0.68±0.25	0.99±0.11	0.98±0.34	1.28±0.19
Caspase 1	1582623	10.69±4.14	2.53±0.52*	5.33±2.36	1.82±0.50	0.72±0.41	0.85±0.05	0.81±0.27	0.79±0.03
Cell structure and mobility									
Smooth muscle gamma actin	1586210	2.39±0.44	3.39±0.52**	6.45±3.60*	5.66±2.95	1.16±0.21	1.37±0.22	1.64±0.48	1.88±0.37
Skeletal myosin light chain 2	1583107	0.50±0.03*	0.66±0.03**	0.51±0.05*	0.66±0.04**	1.16±0.16	1.18±0.10	1.01±0.27	1.32±0.32
Extracellular matrix									
TIMP-1	1582383	7.62±2.36	5.85±1.72*	8.91±3.57	6.53±1.84*	1.28±0.88	1.01±0.45	1.23±0.46	1.09±0.09
MMP-2	1582764	1.33±0.31	1.07±0.18	8.17±1.38**	4.46±0.34**	1.55±0.64	1.15±0.14	2.36±1.23	2.01±0.51
Fibronectin	1582768	20.19±7.15*	10.70±2.33**	23.67±7.68**	16.20±2.62**	1.68±0.84	1.49±0.32	2.04±0.46	2.75±0.42
Collagen alpha 1(III) chain precursor	1591762	3.77±0.98	2.27±0.61	36.93±7.83**	20.18±1.54**	1.41±0.80	1.83±0.61	2.75±1.11	4.46±1.11
DNA–RNA synthesis									
EF-TFIIS	1585822	0.64±0.07	0.65±0.09*	0.52±0.14	0.51±0.06**	1.55±0.48	0.88±0.04	1.06±0.33	0.74±0.03*
EF-TU	1583725	1.26±0.14	1.25±0.14	0.66±0.10	0.72±0.09*	1.50±0.34	1.00±0.07	0.85±0.16	0.80±0.09
Immunity									
Von Willebrand factor (VWF)	1582505	1.43±0.20	1.42±0.24	2.63±0.35**	2.54±0.18*	2.11±0.58	1.21±0.33	2.78±0.51	1.91±0.27
Integrin beta-1 binding protein 2	1591346	2.41±0.32**	1.97±0.21**	1.33±0.07	1.09±0.05	0.79±0.29	0.57±0.05*	0.67±0.17	0.62±0.04*
FLAP	1601853	12.83±4.28*	3.32±0.58**	12.37±3.47*	4.70±0.74**	1.23±0.52	1.19±0.10	1.02±0.27	2.47±0.29*
IL1-Ra	1582494	5.80±2.36	3.42±1.15	15.24±8.58	9.94±3.36*	0.37±0.18	0.60±0.05	1.49±0.88	0.65±0.05
Ion transport									
ERG	1582833	0.57±0.04	0.76±0.04**	0.87±0.13	1.00±0.07	1.85±0.45	1.31±0.03*	1.13±0.19	1.33±0.18
KChIP-2	1582775	0.31±0.07**	0.36±0.06**	0.13±0.03*	0.17±0.03**	1.14±0.35	0.57±0.12	0.72±0.17	0.48±0.04
Metabolism									
Cytochrome-*c* oxidase subunit Via	1583218	2.26±0.43	1.84±0.15**	1.75±0.14**	1.64±0.04**	0.99±0.21	0.96±0.13	1.21±0.25	1.15±0.07

*$P<0.05$. **$P<0.01$ versus sham dogs. 24-hour LA; 2-week LA = left atrial tissue from dogs ventricular-tachypaced for 24 h and 2 weeks respectively; 24-hour LV and 2-week LV = left-ventricular tissue from dogs ventricular-tachypaced for 24 h and 2 weeks respectively.
TIMP = Tissue inhibitor of metalloproteinase; MMP = Matrix Metalloproteinase; EF = Elongation factor; FLAP = 5-lipoxygenase activating protein; IL1 = interleukin-1; ERG = ether-a-go-go related gene; KChIP = K^+-channel interacting protein.

genes encoding electron-chain transport enzymes were altered (primarily down-regulated) by VTP, with all 5 complexes affected in LA tissue but only complexes I and II affected in LV, with 7 and 2 genes significantly down-regulated respectively. In contrast to the Krebs cycle and complexes I and II of electron-chain transport, which were significantly altered in LV, genes encoding glycolytic enzymes were affected only in LA (On-line Fig. 6). Sixteen genes were affected by VTP in the LA, with similar numbers altered at 24 h and 2 weeks of VTP.

4. Discussion

In this study, we compared mRNA expression changes in LA and LV over two weeks of VTP-induced CHF in the dog. The results show striking discrepancies in the atrial versus ventricular response, time-dependant evolution of expression changes and alterations in chamber-selective gene-expression profiles.

4.1. LA–LV gene-expression differences with and without HF

A variety of investigators have noted substantial gene-expression differences between atrial and ventricular tissues of mouse [22], dog [23] and human hearts [12,24,25]. A particularly detailed analysis was reported by Barth et al. [24]. They used a commercially-available microarray directed towards 11,740 transcripts to compare gene-expression between 17 right-atrial (RA) appendages from patients undergoing open-heart surgery with LV transmural tissue-slices from 5 non-failing donor hearts. At a false-discovery rate of <0.03, they found differences in 6,274 transcripts (53% of probe-sets available), with 3,300 being more strongly-expressed in atrium and 2,974 in ventricle. They noted stronger expression of genes related to metabolism in LV and a predominance of genes involved in signal transduction and apoptosis in atrium, findings similar to ours. The overall number of atrial–ventricular differences that they observed is slightly more than what we noted here with a somewhat stricter statistical-significance cut-off and the balance between atrial-predominant and ventricular-predominant genes is similar.

We are not aware of previous studies that analyzed the evolution of atrial–ventricular gene-expression differences with the development of CHF. Barth et al noted that in atria of AF patients upregulation occurred predominantly in "ventricular-predominant" genes and down-regulation in "atrial-predominant" genes, producing a "ventricularization" of the atrial gene-expression profile [12]. We noted a similar type of phenomenon, with the number of statistically-significant LA–LV gene-expression differences decreasing with the advent of CHF (Fig. 3). A total of 1273 of the 1599 genes with significantly-differential LA–LV expression in shams were no longer significantly different at 2-wk VTP, presumably mostly because of LA expression changes (since few statistically-significant changes occurred in LV). On the other hand, 1086 genes that were LA–LV equivalent in shams showed significant LA–LV differences at 24-hour VTP and 576 at 2-week VTP. Thus, it seems that CHF greatly reduces the LA–LV gene-expression differences that are present in the normal heart, only to replace them by a range of chamber-selective pathological responses.

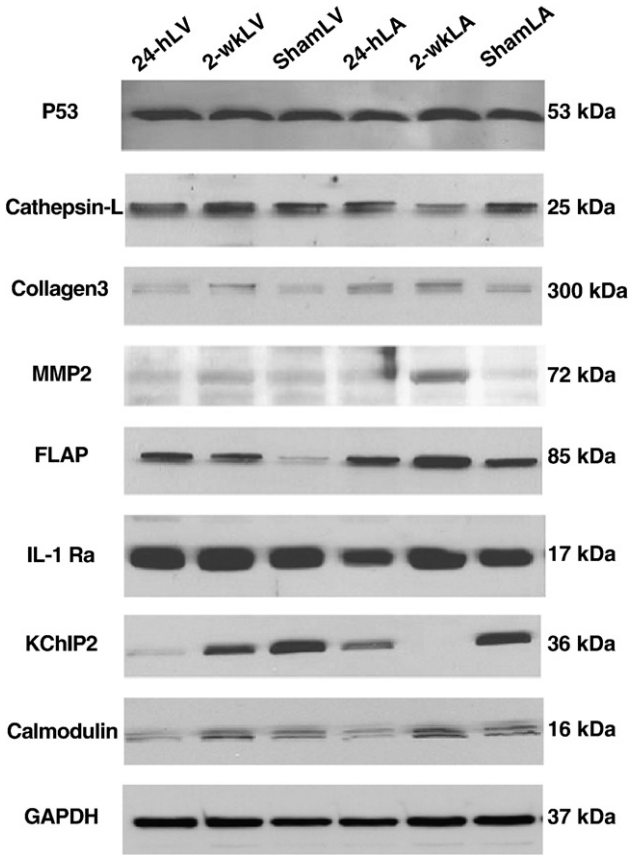

Fig. 6. Examples of Western blots for 8 proteins studied to compare protein versus mRNA expression changes, along with an immunoblot for the internal control (GAPDH). All gels were run with lanes in an identical order except those for MMP2, which therefore had to be cut from one original gel and pasted in the appropriate order to match the other protein samples shown. Results for all proteins other than MMP2 are taken from single original gels in intact sequence.

4.2. Gene-expression changes in CHF and differential atrial–ventricular response

CHF causes deterioration in cardiac function and significant reprogramming of cardiac gene-expression. Barrans et al. found over 100 of 10,848 expressed sequence–sequence tags to be changed >1.5-fold in LVs of patients with end-stage cardiomyopathy [26]. Relatively few studies have compared atrial versus ventricular gene-expression changes in CHF. Kääb et al. studied human atrial and ventricular gene-expression response differences by comparing 8 terminally-failing ischemic and dilated cardiomyopathic hearts with 5 non-failing donor hearts via microarray analysis [4]. They found about twice as many significantly-changed genes at the atrial level, and noted a predominance of down-regulated genes (103) compared to upregulated (13) in the ventricles. We similarly found a predominance of gene down-regulation in the LV (Fig. 2B), and although there was a much greater quantitative discrepancy we also noted a stronger gene-response to CHF in the atrium versus ventricle. Kb et al. noted that only ~7% of significantly-changed genes were common to both atria and ventricles, a figure of a similar order to what we observed (~2%).

We were unable to identify studies comparing directly atrial with ventricular gene-expression profile changes in animal CHF models. Gao et al. used human gene microarrays to compare ventricular gene-expression between 4 normal dogs and 4 dogs with terminal CHF caused by 4-wk VTP [6] (atrial gene-expression was not assessed). They noted a large number of statistically-significant ventricular gene-expression changes in CHF, over 1000, once again with about 20 times as many genes (971) down- as up-(49) regulated. Like us, they found down-regulation of metabolic pathways and transport genes. The discrepancy in the number of statistically-significant ventricular gene-expression changes between their study and ours is likely due to the fact that they studied dogs with terminal CHF after 4-wk VTP (LVEDP~30), whereas our dogs had less severe cardiac decompensation with a maximum of 2-wk VTP.

The differential atrial–ventricular gene-expression response to VTP-induced CHF that we noted in the present study is coherent with markedly different atrial versus ventricular tissue responses that we detailed with the same dog model in a previous report [5]. In that study, the LA showed much stronger changes in terms of leukocyte-infiltrative inflammatory response, total and apoptotic cell-death rate and tissue fibrosis than LV. There was also a differential evolution of histological changes. Acute responses (white-cell infiltration and cell-death) peaked in the LA at 24 h and then returned to baseline over 5 weeks, in contrast to fibrosis which increased progressively over 5 weeks. In the LV, white-cell infiltration and cell-death were less intense than in LA (5–10 fold) but were less transient, remaining at about the same level or increasing from 24-hour to 5-week VTP.

4.3. Extracellular matrix remodeling

Extracellular matrix (ECM) remodeling is of particular importance in creating the AF substrate in CHF [2,3,5,7–10]. ECM-related genes showed dramatically-different remodeling in LA versus LV. About 150 LA ECM-transcripts were significantly altered at 2-wk VTP, compared to 2 at the LV level. Some notable examples include highly-significant ~20 and ~65-fold increases in LA collagen-3 and collagen-1 genes respectively, versus statistically non-significant 4.5 and 7.9-fold increases in the LV. LA fibronectin gene-expression increased significantly by ~11 and ~16-fold at 24-hour and 2-week VTP, while LV fibronectin averaged ~1.5 and ~2.7 times sham values at 24-hour and 2-week VTP (P=NS for both). Tissue-inhibitor of matrix metalloprotease-1 (TIMP-1) was ~6-fold increased in LA at 24-hour but not 2-week VTP, whereas matrix metalloproteinase-9 (MMP9) was increased ~6-fold at 2-week but not 24-hour VTP; neither were significantly altered in LV. These important ECM-gene-expression differences parallel and account for the much greater fibrotic response previously observed in LA versus LV tissue in this model [5].

4.4. Metabolism

The failing myocardium is characterized by an important reduction in high-energy phosphate and phosphotransferase enzymes such as creatine-kinase. The single largest group of LV gene-changes occurred in genes involved in metabolism. Although most metabolism-related genes were down-regulated, the creatine-kinase B (CK-B) gene showed striking 8-fold up-regulation at 2-wk VTP. The creatine-kinase isoenzyme CK-B is involved in the formation of the active forms CK-BB and CK-MB. Previous studies have shown that the activity of the CK-MM isoform is decreased by ~30%, but the activity of the CK-MB isoform is at least two-fold higher in the failing heart, correlating with a 5-fold increase in CK-B isoenzyme in the ventricles [27,28].

Gao et al noted down-regulation of ventricular genes involved in energy production in end-stage VTP-induced CHF [6]. We also observed marked decreases in components of the respiratory-chain complex. NADH dehydrogenase Fe–S proteins 3 and 8 (CI), succinate dehydrogenase complex (CII) and ubiquinol-cytochrome *C* oxydoreductase (CIII) all showed reduced expression at 2-wk VTP in both LA and LV. NADH and succinate dehydrogenase produce reduction reactions that create a H^+-electrochemical gradient toward the inner mitochondrial membrane. These H^+-ions are driven back into the mitochondrial matrix via ATP-synthase and allow the production of ATP. Respiratory-chain systems also play an important role in regulating oxidative stress and thereby apoptosis, which is of great importance in CHF progression [29,30].

Table 3
Comparison between microarray and western blot results (Fold-changes)

Protein	Gene ID	Group	Microarray	Western blot (mean)	SEM	P versus CTL
Calmodulin	1604374	24-hr LA	0.99	1.35*	0.08	0.014
Signal transduction		2-wk LA	1.19	1.37	0.25	0.111
		24-hr LV	1.27	1.22	0.21	0.172
		2-wk LV	**1.89***	**1.65***	**0.151**	**0.017**
P53	1582452	24-hr LA	1.06	0.86	0.15	0.271
Apoptosis		2-wk LA	0.97	0.98	0.29	0.922
		24-hr LV	1.16	0.97	0.1	0.368
		2-wk LV	1.12	1	0.13	0.488
Cathepsin L	1583225	24-hr LA	0.59**	0.56	0.23	0.082
Apoptosis		2-wk LA	1.21	0.34*	0.15	0.004
		24-hr LV	0.78	0.96	0.15	0.381
		2-wk LV	1.07	1.06	0.06	0.184
Collagen 3 α 1	1591762	24-hr LA	2.27	0.87	0.34	0.647
Extracellular matrix		**2-wk LA**	**20.18****	**1.79***	**0.29**	**0.035**
		24-hr LV	1.83	0.91	0.05	0.075
		2-wk LV	4.46	1.09	0.15	0.267
MMP-2	1582764	24-hr LA	1.07	1.73	1.13	0.443
Extracellular matrix		**2-wk LA**	**4.46****	**6.16***	**2.4**	**0.047**
		24-hr LV	1.15	1.27	0.15	0.088
		2-wk LV	2.01	1.22	0.25	0.195
FLAP	1601853	**24-hr LA**	**3.32****	**2.16***	**0.45**	**0.037**
Immunity		**2-wk LA**	**4.70****	**4.57***	**1.45**	**0.048**
		24-hr LV	1.19	0.96	0.12	0.37
		2-wk LV	2.47*	1.38	0.18	0.063
IL1-RA	1582494	24-hr LA	3.42	1.46*	0.14	0.026
Immunity		2-wk LA	9.94*	1.50*	0.18	0.032
		24-hr LV	**0.6**	**0.57***	**0.07**	**0.01**
		2-wk LV	0.65	0.62*	0.06	0.013
KCHIP2	1582775	**24-hr LA**	**0.36****	**0.24***	**0.07**	**0.009**
Transport		**2-wk LA**	**0.17****	**0.12***	**0.01**	**0**
		24-hr LV	0.57	0.44*	0.08	0.007
		2-wk LV	0.48	0.35*	0.06	0.002

*Statistically significant difference; *P* versus CTL indicates *P*-value for difference from control protein expression (Western blot). Microarray results, **Statistically significant $Q<1$, *$Q<5$. Dark grey = significant on both Genechip and Western; Light Grey = non-significant on both. 24-hr LA; 2-wk LA = left atrial tissue from dogs ventricular-tachypaced for 24 h and 2 weeks respectively; 24-hr LV and 2-wk LV = left-ventricular tissue from dogs ventricular-tachypaced for 24 h and 2 weeks respectively.

4.5. Ca^{2+}-signalling

Remodeling of Ca^{2+}-handling is emerging as an important pathophysiological paradigm in atrial and ventricular arrhythmogenesis related to heart disease [31]. Key components include the Ca^{2+}-calmodulin-dependent protein-kinase-II (CaMKII) and ryanodine receptor-FKBP12/12.6 systems [31–33]. Of the relatively small number of LV genes up-regulated at 2-week VTP, FKBP12 and calmodulin are prominent. FKBP12 was also increased in LA at 24-hour and 2-week VTP.

4.6. Pathway analyses

A number of signalling and metabolic pathways were significantly altered by VTP. In keeping with evidence for an important role of MAPK signalling at the protein level [5,13,17], many mRNA species encoding components of the MAPK system were affected and most of them were upregulated (On-line Fig. 1). Interestingly, transcripts encoding the small G-protein Rac1 were the most strongly upregulated, increased ~3.7-fold at 24 h and 1.9-fold at 2 weeks. There is evidence for an important role of Rac1 in the pathophysiology of AF [34,35], and

since Rac1 is an important target of statin action, its alteration may account for the beneficial effects of statins in CHF-associated atrial structural remodeling [35,36].

Apoptosis appears to play an important role in CHF-associated AF [5,13,37], and pathways related to apoptosis, both directly (On-line Fig. 2) and via the ubiquitin–proteasome system (On-line Fig. 3) were significantly affected. Elements of both systems involved in endoplasmic reticulum stress responses were altered, consistent with evidence for an important role of oxidant stress in CHF [30] and AF [31]. The extensive LA changes observed at multiple levels in the ubiquitin–proteasome system are consistent with a hypothesized role of the system in CHF [20], and with evidence for hyperubiquinated proteins in terminally-failing human hearts [38].

Genomic analysis at the ventricular level was striking for the relative paucity of changes observed, with the notable exception of specific metabolic pathways. These observations are in keeping with the prominent role of metabolic changes in the pathophysiology of CHF [39]. It must also be noted that metabolic derangements related to high LV metabolic demands at a heart rate of 240 bpm are likely to be central to the development of CHF in the VTP model. The down-regulation of genes encoding enzymes in the first part of the Krebs cycle may favour the use of 2-ketoglutarate derived from glutamate in energy metabolism. Downregulation of mitochondrial electron-chain enzyme genes linked to complex II may be a response to minimize free radical formation by reverse electron flow.

4.7. Potential significance

The present study is, to our knowledge, the first systematic assessment of atrial versus ventricular mRNA expression remodeling differences in an animal CHF model. In addition, we made comparisons over time that allowed us to identify the dynamic development of gene-expression changes. Our findings show a striking difference between the LA and LV response, which sheds light on previously-noted differences between the atrial and ventricular neurohumoral responses, apoptosis, inflammation, cell-death and fibrosis in the same model [5]: the LA changes peaked much earlier and were up to 10-fold greater in magnitude compared to LV [5]. Taken together with the results of previous work, our findings suggest that the rapidly-developing CHF-associated with tachycardiomyopathy places a particularly great burden on the atria. The differential gene-response must reflect strongly-induced programs of atrial adaptation to a very major stress. Further work designed to clarify the atrial-remodeling programs may help in the development of novel approaches to preventing atrial arrhythmogenic substrate development, an important evolving theme in AF therapeutics [40]. The relatively limited number of LV gene-expression changes likely reflects a greater capacity of the ventricles to cope with a tachycardic stress and is consistent with previous observations of dramatic ventricular recovery upon termination of tachypacing. Interestingly, although hemodynamic function and ventricular dimensions recover completely following the cessation of VTP, atrial structural remodeling remains, as does a persistent substrate that can sustain AF [8,9].

4.8. Potential limitations

The time-points we examined were selected based on previous evidence for important early-phase changes at 24 h and near steady-state late-phase changes at 2 weeks of VTP-induced remodeling, particularly at the atrial level [5,13]. However, other time-points would be interesting to study, particularly as ventricular function deteriorates rapidly towards terminal CHF. The model that we used (VTP) is widely-employed and mimics well some forms of clinical CHF [41]; however, observations of LA versus LV remodeling in other clinically-relevant experimental paradigms might provide different results and would be of great interest. With the model that we used, CHF develops within 2 weeks and becomes terminal in 4–5 weeks. This time-course is much faster than that of many clinical forms of CHF, which often evolve over many months to years. This limitation, which also applies to most other animal models of CHF, needs to be considered in extrapolating our results to clinical contexts.

We used a statistical cut-off for VTP-induced changes in the present paper of $q<5$, implying a false-positive rate of 5% (equivalent to a P-value of $P<0.05$), whereas in our previous study of atrial-cardiomyocyte genomics with CHF versus atrial-tachypacing the cut-off was a q-value <1, implying a false-positive rate of 1% or $P<0.01$ [14]. This approach explains the larger number of statistically-significant changes we noted at the atrial level in this study, and would of necessity have increased the number of false-positive detections. We were forced to use the less restrictive statistical criterion because with the stricter cut-off, there were no statistically-significant VTP-induced changes detected in the LV.

We obtained a detailed portrait of changes at the mRNA level for a wide range of genes in the LA and LV of dogs subjected to VTP for varying periods. This clearly, however, represents only a small part of a much larger picture, potentially including changes in protein production, processing and trafficking. Much more work will be needed to identify the additional elements required for a complete picture of the dynamic processes governing atrial and ventricular remodeling over time during the development of CHF.

Acknowledgments

Supported by the Canadian Institutes of Health Research (Grant numbers MOP 68929 and MGP 6957) and the Quebec and Heart and Stroke Foundation. SC received a Heart and Stroke Foundation of Canada (HSFC) studentship and Sabrina Le Bouter FRSQ-INSERM and HSFC fellowships. The authors thank Nathalie L'Heureux, Chantal Maltais and Chantal St-Cyr for technical help, France Thriault for secretarial support and Christine Des Rosiers, PhD, for helpful discussions regarding metabolic remodeling.

Appendix A. Supplementary data

Supplementary data associated with this article can be found, in the online version, at doi:10.1016/j.yjmcc.2008.08.007.

References

[1] Jessup M, Brozena S. Heart failure. Review. N Engl J Med 2003;348:2007–18.
[2] Nattel S, Shiroshita-Takeshita A, Cardin S, Pelletier P. Mechanisms of atrial remodeling and clinical relevance. Curr Opin Cardiol 2005;20:21–5.
[3] Brundel BJ, Melnyk P, Rivard L, Nattel S. The pathology of atrial fibrillation in dogs. J Vet Cardiol 2005;7:121–9.
[4] Kääb S, Barth AS, Margerie D, Dugas M, Gebauer M, Zwermann L, et al. Global gene expression in human myocardium-oligonucleotide microarray analysis of regional diversity and transcriptional regulation in heart failure. J Mol Med 2004;82:308–16.
[5] Hanna N, Cardin S, Leung TK, Nattel S. Differences in atrial versus ventricular remodeling in dogs with ventricular tachypacing-induced congestive heart failure. Cardiovasc Res 2004;63:236–44.
[6] Gao Z, Xu H, DiSilvestre D, Halperin VL, Tunin R, Tian Y, et al. Transcriptomic profiling of the canine tachycardia-induced heart failure model: global comparison to human and murine heart failure. J Mol Cell Cardiol 2006;40:76–86.
[7] Nattel S, Shiroshita-Takeshita A, Brundel B, Rivard L. Mechanisms of atrial fibrillation: lessons from animal models. Prog Cardiovasc Dis 2005;48:9–28.
[8] Shinagawa K, Shi YF, Tardif JC, Leung TK, Nattel S. Dynamic nature of the atrial fibrillation substrate during development and reversal of the heart failure in dogs. Circulation 2002;105:2672–8.
[9] Cha TJ, Ehrlich JR, Zhang L, Shi YF, Tardif JC, Leung TK, et al. Dissociation between ionic remodelling and ability to sustain atrial fibrillation during recovery from experimental congestive heart failure. Circulation 2004;109:412–8.
[10] Li D, Fareh S, Leung TK, Nattel S. Promotion of atrial fibrillation by heart failure in dogs: atrial remodeling of a different sort. Circulation 1999;100:87–95.
[11] Li D, Melnyk P, Feng J, Wang Z, Petrecca K, Shrier A, et al. Effects of experimental heart failure on atrial cellular and ionic electrophysiology. Circulation 2000;101:2631–8.
[12] Barth AS, Merk S, Arnoldi E, Zwermann L, Kloos P, Gebauer M, et al. Reprogramming of the human atrial transcriptome in permanent atrial fibrillation: expression of a ventricular-like genomic signature. Circ Res 2005;96:1022–9.
[13] Cardin S, Li D, Thorin-Trescases N, Leung TK, Thorin E, Nattel S. Evolution of the atrial fibrillation substrate in experimental congestive heart failure: angiotensin-dependent and independent pathways. Cardiovasc Res 2003;60:315–25.

[14] Cardin S, Libby E, Pelletier P, Le Bouter S, Shiroshita-Takeshita A, Le Meur N, et al. Contrasting gene expression profiles in two canine models of atrial fibrillation. Circ Res 2007;100:425–33.
[15] Xiao L, Zhang L, Han W, Wang Z, Nattel S. Sex-based transmural differences in cardiac repolarization and ionic-current properties in canine left ventricles. Am J Physiol (Heart Circ Physiol) 2006;291:H570–580.
[16] Dahlquist KD, Salomonis N, Vranizan K, Lawlor SC, Conklin BR. GenMAPP, a new tool for viewing and analyzing microarray data on biological pathways. Nat Genet 2002;31:19–20.
[17] Li D, Shinagawa K, Pang L, Leung TK, Cardin S, Wang Z, et al. Effects of angiotensin-converting enzyme inhibition on the development of the atrial fibrillation substrate in dogs with ventricular tachypacing-induced congestive heart failure. Circulation 2001;104:2608–14.
[18] Liao PC, Tan SK, Lieu CH, Jung HK. Involvement of endoplasmic reticulum in paclitaxel-induced apoptosis. J Cell Biochem 2008;104:1509–23.
[19] Roubille F, Combes S, Leal-Sanchez J, Barrre C, Cransac F, Sportouch-Dukhan C, et al. Myocardial expression of a dominant-negative form of Daxx decreases infarct size and attenuates apoptosis in an in vivo mouse model of ischemia/reperfusion injury. Circulation 2007;116:2709–17.
[20] Powell SR. The ubiquitin–proteasome system in cardiac physiology and pathology. Am J Physiol (Heart Circ Physiol) 2006;291:H1–H19.
[21] Patterson C, Ike C, Willis 4th PW, Stouffer GA, Willis MS. The bitter end: the ubiquitin–proteasome system and cardiac dysfunction. Circulation 2007;115: 1456–63.
[22] Tabibiazar R, Wagner RA, Liao A, Quertermous T. Transcriptional profiling of the heart reveals chamber-specific gene expression patterns. Circ Res 2003;93: 1193–201.
[23] Zhao XS, Gallardo TD, Lin L, Schageman JJ, Shohet RV. Transcriptional mapping and genomic analysis of the cardiac atria and ventricles. Physiol Genomics 2002;12: 53–60.
[24] Barth AS, Merk S, Arnoldi E, Zwermann L, Kloos P, Gebauer M, et al. Functional profiling of human atrial and ventricular gene expression. Pflugers Arch 2005;450: 201–8.
[25] Ellinghaus P, Scheubel RJ, Dobrev D, Ravens U, Holtz J, Huetter J, et al. Comparing the global mRNA expression profile of human atrial and ventricular myocardium with high-density oligonucleotide arrays. J Thorac Cardiovasc Surg 2005;129: 1383–90.
[26] Barrans JD, Allen PD, Stamatiou D, Dzau VJ, Liew CC. Global gene expression profiling of end-stage dilated cardiomyopathy using a human cardiovascular-based cDNA microarray. Am J Pathol 2002;160:2035–43.
[27] Nascimben L, Ingwall JS, Pauletto P, Friedrich J, Gwathmey JK, Saks V, et al. Creatine kinase system in failing and nonfailing human myocardium. Circulation 1996;94: 1894–901.
[28] Heinke MY, Wheeler CH, Yan JX, Amin V, Chang D, Einstein R, et al. Changes in myocardial protein expression in pacing-induced canine heart failure. Electrophoresis 1999;20:2086–93.
[29] Ide T, Tsutsui H, Kinugawa S, Utsumi H, Kang D, Hattori N, et al. Mitochondrial electron transport complex I is a potential source of oxygen free radicals in the failing myocardium. Circ Res 1999;85:357–63.
[30] Hare JM. Oxidative stress and apoptosis in heart failure progression. Circ Res 2001; 89:198–200.
[31] Nattel S, Maguy A, Le Bouter S, Yeh YH. Arrhythmogenic ion-channel remodeling in the heart: heart failure, myocardial infarction, and atrial fibrillation. Physiol Rev 2007;87:425–56.
[32] Ai X, Curran JW, Shannon TR, Bers DM, Pogwizd SM. Ca^{2+}/calmodulin-dependent protein kinase modulates cardiac ryanodine receptor phosphorylation and sarcoplasmic reticulum Ca^{2+} leak in heart failure. Circ Res 2005;97:1314–22.
[33] Anderson ME. Calmodulin and the philosopher's stone: changing Ca^{2+} into arrhythmias. J Cardiovasc Electrophysiol 2002;13:195–7.
[34] Adam O, Frost G, Custodis F, Sussman MA, Schäfers HJ, Böhm M, et al. Role of Rac1 GTPase activation in atrial fibrillation. J Am Coll Cardiol 2007;50:359–67.
[35] Tsai CT, Lai LP, Kuo KT, Hwang JJ, Hsieh CS, Hsu KL, et al. Angiotensin II activates signal transducer and activators of transcription 3 via Rac1 in atrial myocytes and fibroblasts: implication for the therapeutic effect of statin in atrial structural remodeling. Circulation 2008;117:344–55.
[36] Shiroshita-Takeshita A, Brundel BJ, Burstein B, Leung TK, Mitamura H, Ogawa S, et al. Effects of simvastatin on the development of the atrial fibrillation substrate in dogs with congestive heart failure. Cardiovasc Res 2007;74:75–84.
[37] Aimé-Sempé C, Folliguet T, Rcker-Martin C, Krajewska M, Krajewska S, Heimburger M, et al. Myocardial cell death in fibrillating and dilated human right atria. J Am Coll Cardiol 1999;34:1577–86.
[38] Weekes J, Morrison K, Mullen A, Wait R, Barton P, Dunn MJ. Hyperubiquitination of proteins in dilated cardiomyopathy. Proteomics 2003;3:208–16.
[39] Ventura-Clapier R, Garnier A, Veksler V. Energy metabolism in heart failure. J Physiol 2004;555(Pt 1):1–13.
[40] Camm AJ. Medical management of atrial fibrillation: state of the art. J Cardiovasc Electrophysiol 2006;17(Suppl 2):S2–6.
[41] Moe GW, Armstrong P. Pacing-induced heart failure: a model to study the mechanism of disease progression and novel therapy in heart failure. Cardiovasc Res 1999;42:591–9.